Title
Rapid Broad-Spectrum Analgesia through Activation of Peroxisome Proliferator-Activated Receptor-α

Journal
Journal of Pharmacology and Experimental Therapeutics, 319(3)

ISSN
0022-3565

Authors
LoVerme, Jesse
Russo, Roberto
La Rana, Giovanna
et al.

Publication Date
2006-12-01

DOI
10.1124/jpet.106.111385

0022-3565/06/3193-1051–1061$20.00
THE JOURNAL OF PHARMACOLOGY AND EXPERIMENTAL THERAPEUTICS
JPET 319:1051–1061, 2006

Vol. 319, No. 3
111385/3157528
Printed in U.S.A.

Rapid Broad-Spectrum Analgesia through Activation of Peroxisome Proliferator-Activated Receptor-α

Jesse LoVerme, Roberto Russo, Giovanna La Rana, Jin Fu, Jesse Farthing, Giuseppina Mattace-Raso, Rosaria Meli, Andrea Hohmann, Antonio Calignano, and Daniele Piomelli

Department of Pharmacology and the Center for Drug Discovery, University of California, Irvine, California (J.L., J.F. D.P.); Department of Experimental Pharmacology, University of Naples, Naples, Italy (R.R., G.L., G.M.R., R.M., A.C.); and Department of Psychology, University of Georgia, Athens, Georgia (J.F., A.H.)

Received July 24, 2006; accepted September 21, 2006

ABSTRACT

Severe pain remains a major area of unmet medical need. Here we report that agonists of the nuclear receptor PPAR-α (peroxisome proliferator-activated receptor-α) suppress pain behaviors induced in mice by chemical tissue injury, nerve damage, or inflammation. The PPAR-α agonists GW7647 [2-(4-(2-(1-cyclohexanebutyl)-3-cyclohexylureido)ethyl)phenylthio)-2-methylpropionic acid], Wy-14643 [4-chloro-6-(2,3-xylidino)-2-pyrimidinylthioacetic acid], and palmitoylethanolamide (PEA) reduced nocifensive behaviors elicited in mice by intraplantar (i.pl.) injection of formalin or i.p. injection of magnesium sulfate. These effects were absent in PPAR-α-null mice yet occurred within minutes of agonist administration in wild-type mice, suggesting that they were mediated through a transcription-independent mechanism. Consistent with this hypothesis, blockade of calcium-operated IK_{ca} ($K_{Ca}3.1$) and BK_{ca} ($K_{Ca}1.1$) potassium channels prevented the effects of GW7647 and PEA in the formalin test. Three observations suggest that PPAR-α agonists may inhibit nocifensive responses by acting on peripheral PPAR-α. (i) PEA reduced formalin-induced pain at i.pl. doses that produced no increase in systemic PEA levels; (ii) PPAR-α was expressed in dorsal root ganglia neurons of wild-type but not PPAR-α-null mice; and (ii) GW7647 and PEA prevented formalin-induced firing of spinal cord nociceptive neurons in rats. In addition to modulating nociception, GW7647 and PEA reduced hyperalgesic responses in the chronic constriction injury model of neuropathic pain; these effects were also contingent on PPAR-α expression and were observed following either acute or subchronic PPAR-α agonist administration. Finally, acute administration of GW7647 and PEA reduced hyperalgesic responses in the complete Freund's adjuvant and carrageenan models of inflammatory pain. Our results suggest that PPAR-α agonists may represent a novel class of analgesics.

Current therapies do not control safely and effectively severe pain states—a broad spectrum of debilitating conditions that comprises acute, persistent inflammatory, and neuropathic pain. Even widely used drugs, such as opiates (e.g., morphine) or anticonvulsants (e.g., gabapentin), are only active in a fraction of the patient population and produce multiple, often serious, side effects. Thus, despite continuing progress in analgesic drug discovery, the need for therapeutic agents capable of blocking abnormal pain sensation without impairing normal abilities remains largely unmet.

PPAR-α is a nuclear receptor that serves important functions in lipid nutrient utilization and inflammation (Taylor et al., 2002; Kostadinova et al., 2005). Like other members of the nuclear receptor superfamily, PPAR-α is activated

This work was supported by grants form the National Institute on Drug Abuse, the University of California Discovery Program, the Sandler Foundation (to D.P.), by DA14022 and DA14265 (to A.G.H.), and by MIUR (to A.C.).
J.L and R.R. contributed equally to the present study.
Article, publication date, and citation information can be found at http://jpet.aspetjournals.org.
doi:10.1124/jpet.106.111385.

ABBREVIATIONS: PPAR-α, peroxisome proliferator-activated receptor-α; PEA, palmitoylethanolamide; DRG, dorsal root ganglia; K_c, calcium-activated K^+ channels; i.pl., intraplantar; BK_{ca}, large-conductance K_{ca} channels ($K_{ca}1.1$); IK_{ca}, intermediate-conductance K_{ca} channels ($K_{ca}3.1$); OEA, oleoylethanolamide; FAE, fatty-acid ethanolamide; CB_2, cannabinoid receptor type II; WDR, wide dynamic range; PKA, protein kinase A; GW7647, 2-(4-(2-(1-cyclohexanebutyl)-3-cyclohexylureido)ethyl)phenylthio)-2-methylpropionic acid; GAPDH, glyceraldehyde-3-phosphate dehydrogenase; Wy-14643, 4-chloro-6-(2,3-xylidino)-2-pyrimidinylthioacetic acid; GW501516, 2-methyl-4-((4-methyl-2-(4-trifluoromethylphenyl)-1,3-thiazol-5-yl) methylsulfanyl)phenoxy-acetic acid; PEG, polyethylene glycol; SR144528, *N*-[(1*S*)-endo-1,3,3-trimethylbicyclo[2.2.1]heptan-2-yl]-5-(4-chloro-3-methylphenyl)-1-(4-methylbenzyl)pyrazole-3-carboxamide; MS, mass spectrometry; TRAM-34, 1-[(2-chlorophenyl)diphenylmethyl]-1*H*-pyrazole; TRAM-7, 1-tritylpyrrolidine; luc, luciferase; PBS, phosphate-buffered saline; CFA, complete Freund's adjuvant; DMEM, Dulbecco's modified Eagle's medium; WIN-55212-2, (*R*)-(+)-[2,3-dihydro-5-methyl-3-(4-morpholinylmethyl) pyrrolo-[1,2,3-*d*,*e*]-1,4-benzoxazin-6-yl]-1-naphthalenyl-methanone mesylate; AM630, [6-iodo-2-methyl-1-(2-morpholin-4-ylethyl)indol-3-yl]-(4-methoxyphenyl)methanone.

through ligand binding, which causes changes in receptor conformation, heterodimer formation with the 9-*cis*-retinoic acid receptor, recruitment of coactivators into a multiprotein complex, and regulated transcription of responsive genes. Consistent with known roles of PPAR-α, downstream genes engaged by this receptor encode for proteins involved in key aspects of lipid metabolism and inflammation (Kostadinova et al., 2005).

The large multifunctional ligand-binding pocket of PPAR-α allows it to recognize a number of structurally heterogenous molecules, both synthetic and natural. Synthetic PPAR-α agonists comprise low-affinity ligands of moderate selectivity such as the fibrates, which are used in the clinic to treat blood lipid abnormalities (Willson et al., 2000), and high-affinity ligands, which are potent at reducing hyperlipidemia, atherosclerosis, and inflammation in animal models (Kostadinova et al., 2005; Singh et al., 2005). Among natural PPAR-α agonists are nonesterified fatty acids (Willson et al., 2000), oxygenated fatty acids, and fatty-acid ethanolamides (FAE) (Fu et al., 2003).

Palmitoylethanolamide (PEA), a member of the FAE family of PPAR-α ligands, was first identified 50 years ago as a naturally occurring antiinflammatory constituent of plant and animal tissues (LoVerme et al., 2005b). The antiinflammatory effects of this compound result from its ability to activate PPAR-α-dependent gene transcription (LoVerme et al., 2005a) and occur with a time lag of hours (Mazzari et al., 1996). These slow-onset actions are preceded, however, by rapid antinociceptive responses whose time course is incompatible with a transcription-dependent process (Calignano et al., 1998; Jaggar et al., 1998). Despite its potential significance as an analgesic drug target, the molecular mechanism underlying such responses remains unknown.

Materials and Methods

Chemicals

PEA and OEA were prepared as described previously (Astarita et al., 2006). SR144528 was provided by RBI (Natick, MA) as part of the Chemical Synthesis Program of the National Institutes of Health (NIH, Bethesda, MD). All other chemicals were from Tocris (Avonmouth, UK) or Sigma-Aldrich (St. Louis, MO). Fresh drug solutions were prepared immediately before use in a vehicle of 0.9% sterile saline/5% polyethylene glycol (PEG) 400/5% Tween 80, with the exception that glibenclamide was dissolved in 100% dimethyl sulfoxide and apamin, charybdotoxin, and iberiotoxin were dissolved in distilled water.

Animals

All procedures met the NIH guidelines for the care and use of laboratory animals and those of the Italian Ministry of Health (D.L. 116/92). Male Swiss mice were obtained from Charles River (Wilmington, MA), and male Sprague-Dawley rats were obtained from Harlan (Indianapolis, IN). Male wild-type C57BL6 and PPAR-$\alpha^{-/-}$ (B6.129S4-SvJae-Ppara^{tm1Gonz}) mice, previously backcrossed to C57BL6 mice for 12 generations by the vendor, were from Taconic (Germantown, NY), and male Trpv$_1^{-/-}$ mice (B6.129 $\times$ 1-*Trpv1*^{tm1Jul}/J), previously backcrossed to C57BL6 mice for 10 generations by the vendor, were from Jackson Laboratories (Bar Harbor, ME). Heterozygous CB$_2^{-/+}$ mice were kindly provided by Drs. Nancy Buckley and George Kunos. A CB$_2^{-/-}$ colony was established in-house and maintained by heterozygous crossing. All animals were maintained on a 12-h light/12-h dark cycle with free access to water and chow (RMH 2500; Prolab, Framingham, MA).

Surgeries and Treatments

Sciatic nerve ligation was performed essentially following the method of Bennett and Xie (1988). In brief, male Swiss mice were anesthetized with sodium pentobarbital, and the left sciatic nerve was exposed at mid-thigh level through a small incision and ligated at two distinct sites (spaced at a 2-mm interval) with a silk thread. The wound was closed with a single muscle suture and skin clips and dusted with streptomycin powder. In sham-operated animals, the nerve was exposed but not ligated.

Adjuvant-induced arthritis was done by intradermally injecting 0.1 ml of complete Freund's adjuvant (CFA) (*Mycobacterium tuberculosis*; Sigma-Aldrich) into the base of the tail of male Swiss mice. This procedure resulted in significant inflammation of both hindpaws, which was monitored with a mouse plethysmometer (Ugo Basile, Varese, Italy). Carrageenan-induced paw edema was induced by injecting λ-carrageenan (i.pl., 1% weight vol^{-1} in sterile water, 20 μl) into the left hindpaw of Swiss mice. Paw edema was measured by weighing paws excised at the tarsal joints.

Ex Vivo Analyses

RNA Isolation and Complementary DNA Synthesis. We stored lumbar dorsal root ganglion (DRG) (L_4–L_8, excised and combined together for each mouse) tissues in RNA*Later* (Ambion, Austin, TX), extracted total RNA with TRIzol Reagent (Invitrogen, Carlsbad, CA), and quantified it by UV spectroscopy (λ = 260 nm). We synthesized cDNA using oligo(dT) primers (Ambion) and SuperscriptII RNase H-reverse transcriptase (Invitrogen).

Polymerase chain reaction. We performed reverse transcription of total RNA (2 μg) using Oligo(dT)$_{12-18}$ primers (0.2 μg) for 50 min at 42°C and real-time quantitative polymerase chain reaction using an ABI PRISM 7700 sequence detection system (Applied Biosystems, Foster City, CA). We designed primer/probe sets using Primer Express software (Applied Biosystems) and gene sequences obtained from the GenBank database. Primers and fluorogenic probes were synthesized at TibMolbiol (Berlin, Germany). The primer/probe sequences for PPAR-α were forward (F), 5′-CTTCCCAAAGCTCCTTCAAAAA-3′; reverse (R), 5′-CTGCGCATGCTCCGTG-3′; and probe (P), 5′-TGGTGGACCTTCGGCAGCTGG-3′. The primer/probe sequences for glyceraldehyde-3-phosphate dehydrogenase (GAPDH) were forward (F), 5′-TCACTGGCATGGCCTTCC-3′; reverse (R), 5′-GGCGGCAC-GTCACATCC-3′; and probe (P), 5′-TTCCTACCCCCAATGTGTCCGTCG-3′. RNA levels were normalized by using GAPDH as an internal standard, and measurements were conducted as described previously (Fu et al., 2003).

Liquid chromatography-MS analysis. Liquid chromatography-MS analysis of PEA levels were measured using synthetic [^{2}H$_4$]PEA as an internal standard as described previously (Astarita et al., 2006). In brief, tissue samples were subjected to lipid extraction in chloroform/methanol/water (2:1:1), and [^{2}H$_4$]PEA was added as an internal standard. PEA was separated on an 1100-LC system coupled to a 1946A-MS detector (Agilent Technologies, Palo Alto, CA) equipped with an electrospray ionization interface. We used a XDB Eclipse C$_{18}$ column (50 $\times$ 4.6 mm i.d., 1.8 μm; Zorbax; Agilent Technologies) eluted with a rapid gradient of methanol in water (from 85 to 90% methanol in 2.5 min) at a flow rate of 1.5 ml/min. Column temperature was kept at 40°C. MS detection was in the positive ionization mode, capillary voltage was set at 3 kV, and fragmentor voltage was varied from 120 to 140 V. N_2 was used as drying gas at a flow rate of 13 l/min and a temperature of 350°C. Nebulizer pressure was set at 60 psi. We quantified the test compounds monitoring sodium adducts of the molecular ions [M + Na]$^+$ in the selected ion-monitoring mode.

Immunohistochemistry. Mice were anesthetized with halothane and perfused through the left ventricle with saline (300 ml) followed by 4% paraformaldehyde dissolved in 0.1 M PBS (300 ml). The lumbar DRG (L_5–L_6) was excised under a surgical microscope and sliced with a cryostat (Microm, San Diego, CA) into 18-μm-thick sections. The sections were blocked in 4% normal goat serum and

incubated with antibodies for PPAR-α (1:500; Fitzgerald, Concord, MA) or NeuN (1:1000; Chemicon, Temecula, CA) for 24 h at 4°C. The sections were washed with 0.1 M phosphate-buffered saline (PBS) and incubated with secondary antibodies, anti-rabbit IgG Alexa Fluor 488 or anti-mouse IgG Alexa Fluor 546 (1:1000; Molecular Probes, San Diego, CA), for 1 h at room temperature. After additional washing with 0.1 M PBS, the sections were mounted using ProLong Gold anti-fade reagent (Molecular Probes). Images were obtained using a fluorescent microscope.

Receptor Assays

PPAR-α Transactivation Assays. We cultured HeLa cells in Dulbecco's modified Eagle's medium (DMEM), supplemented with fetal bovine serum (10%), and transfected them using FuGENE 6 reagent (3 μl; Roche, Indianapolis, IN) with 1 μg of the luciferase reporter plasmid pFR-luc containing a hygromycin resistance gene (Stratagene, La Jolla, CA). We replaced the medium after 18 h with DMEM containing hygromycin (0.1 mg ml^{-1}; Calbiochem, San Diego, CA) to select for cells expressing the pFR-luc plasmid. After 4 weeks, we isolated the surviving clones and selected a cell line that showed the highest luciferase activity. We generated plasmids containing the ligand-binding domain of human PPAR-α (nucleotides 499-1407), PPAR-β/δ (412–1323), or PPAR-γ (610–1518) fused to the DNA-binding domain of the yeast regulatory protein GAL4 and a neomycin resistance gene under the control of the human cytomegalovirus promoter. We transfected HeLa cells expressing the pFR-luc plasmid with our plasmid constructs using FuGENE 6 (3 μl) reagent. We selected for stably transfected cells using G418 sulfate (0.2 mg ml^{-1}; Calbiochem). These cells were maintained in DMEM containing hygromycin and G418. For transactivation assays, we seeded cells in six-well plates and incubated them for 7 h in DMEM containing appropriate concentrations of test compounds. We used a dual-luciferase reporter assay system (Promega, Madison, WI) and a MIX Microtiter plate luminometer (Dynex, Chantilly, VA) to determine luciferase activity in cell lysates.

Receptor binding. CB_2 receptor binding assays were conducted in membranes of CB_2-overexpressing Chinese hamster ovary cells (PerkinElmer Life and Analytical Sciences, Boston, MA) using [^{3}H]Win-55212-2 (40–60 Ci/mmol, 10 nM; PerkinElmer Life and Analytical Sciences) as ligand binding studies were performed at 25°C with 20 μg of receptor protein in a 20 mM HEPES/1 mM MgCl (pH 7.4) buffer along with [^{3}H]WIN-55212-2 at a concentration of 10 nM. Final assay volume was 500 μl, and the incubation time was 20 min. Receptor-bound [^{3}H]WIN-55212-2 was separated from free [^{3}H]WIN-55212-2 by filtration. The filter paper was washed twice with 200 μl of ice-cold assay buffer and counted by liquid scintillation.

Biochemical Analyses

Immunoblot Analysis. Lumbar spinal cord tissue was weighed and homogenized in Tris-HCl (20 mM, pH 7.5), 10 mM NaF, 150 mM NaCl, 1% Nonidet P-40, 1 mM PMSF, 1 mM Na_3VO_4, leupeptin, and trypsin inhibitor (10 μg/ml). After 1 h, the tissue lysates were subjected to centrifugation ay 100,000*g* for 15 min at 4°C. Protein concentrations were estimated using a Bradford protein assay (Bio-Rad, Hercules, CA) and bovine serum albumin as a standard. Equal

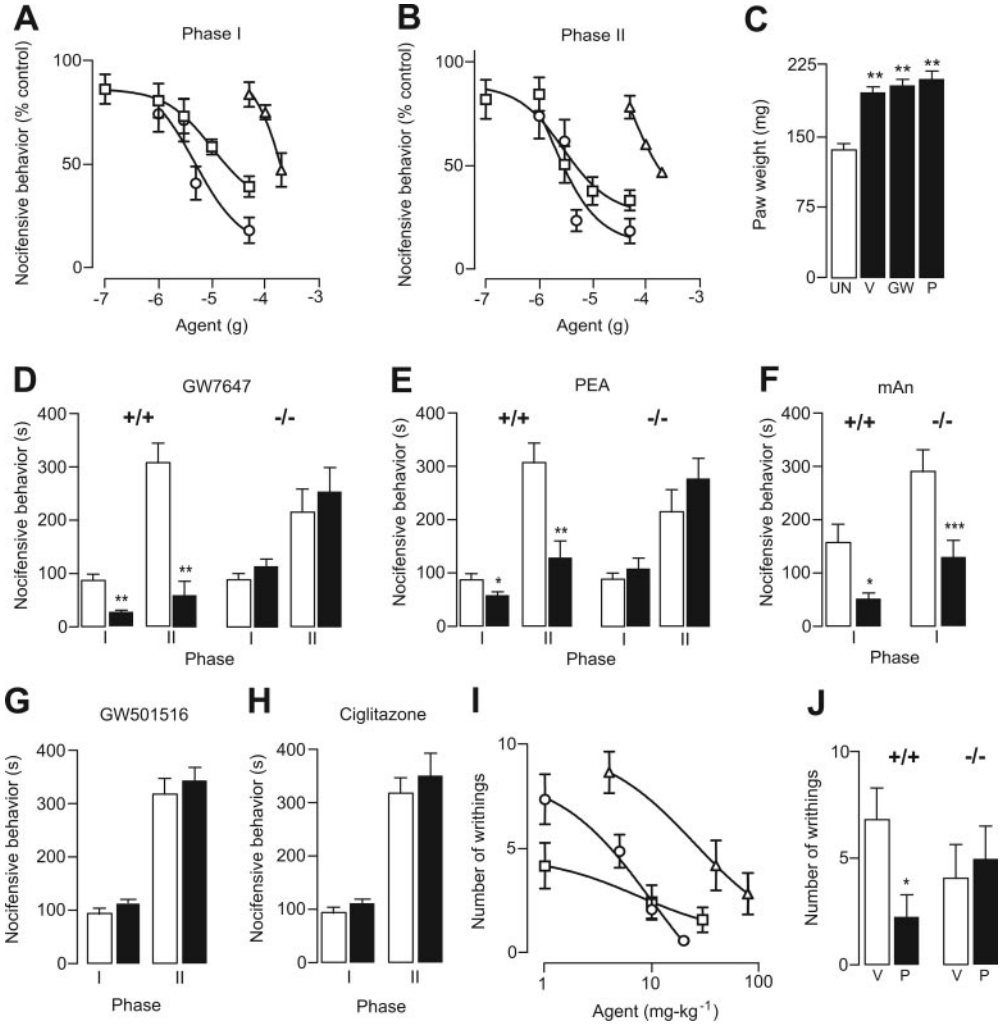

Fig. 1. PPAR-α agonists inhibit tonic nociception in mice. A and B, effects of i.pl. administration of PEA (circles), GW7647 (squares), or Wy-14643 (triangles) on early- (Phase I, 0–15 min) (A) or late-phase (Phase II, 15–45 min) (B) formalin-evoked pain behavior in Swiss mice. Vehicle formalin responses were as follows: Phase I: PEA, 161 ± 19 s; GW7647, 176 ± 12 s; Wy-14643, 137 ± 8 s; Phase II: PEA, 148 ± 21 s; GW7647, 197 ± 18 s; Wy-14643, 154 ± 13 (n = 6–10). C, paw weights measured 45 min after formalin injection in Swiss mice treated with vehicle (V), GW7647 (50 μg i.pl.), or PEA (50 μg i.pl.). UN, paw weight in animals not treated with formalin (n = 5). D to F, effects of vehicle (open bars), GW7647 (closed bars; 50 μg i.pl.) (D), PEA (shaded bars; 50 μg i.pl.) (E), or methanandamide (mAn; closed bars; 50 μg i.pl.) (F) on formalin-evoked nocifensive behavior in wild-type C57BL6 (+/+) or PPAR-$\alpha^{-/-}$ (−/−) mice (n = 6–19). G and H, effects of i.pl. administration of vehicle (open bars), GW501516 (β) (G), or ciglitazone (γ) (H) (each at 50 μg i.pl.) on formalin-evoked pain behavior in wild-type C57BL6 mice (n = 6–10). I, dose-dependent effects of s.c. administration of PEA (circles), GW7647 (squares), or Wy-14643 (triangles) on magnesium sulfate-evoked writhing in Swiss mice (n = 8). J, effects of vehicle (V) or PEA (P, 20 mg kg^{-1} s.c.) on magnesium sulfate writhing in wild-type C57BL6 (+/+) and PPAR-$\alpha^{-/-}$ (−/−) mice (n = 10). (*, $P < 0.05$; **, $P < 0.01$; ***, $P < 0.001$) versus V.

amounts of protein (20 μg) were dissolved in Laemmli sample buffer, boiled for 5 min, subjected to SDS-polyacrylamide gel electrophoresis (8% polyacrylamide), and transferred onto nitrocellulose membranes at 240 mA for 40 min at room temperature. The filter was blocked with PBS, 5% nonfat dried milk for 40 min at room temperature and incubated overnight at 4°C with rabbit primary antibodies to phosphorylated Ser^{96} protein kinase A (PKA) regulatory subunit (1:300; Upstate Biotechnology, Lake Placid, NY), PKA-α catalytic subunit (1:20,0000; Santa Cruz Biotechnology, Santa Cruz, CA), or α-tubulin (1:8000; Sigma-Aldrich) at a dilution of 1:500 for 1 h at room temperature in PBS, 5% nonfat dried milk, and 0.1% Tween 80. After washing and incubation with peroxidase conjugate secondary antibody (anti-rabbit IgG-horseradish, 1:2000 dilution) for 1 h at room temperature, the blots were developed using enhanced chemiluminescence detection reagents (Amersham, Buckinghamshire, UK) according to the manufacturer's instructions and exposed to Kodak X-OMAT films (Eastman Kodak Co, Rochester, NY). The films were scanned and densitometrically analyzed with a model GS-700 imaging densitometer.

Behavioral Assays

Tonic Nociception. We injected formalin (5% formaldehyde in sterile saline, 10 μl) into the plantar surface of mice using a 27-gauge needle fitted to a microsyringe. Vehicle or drugs were dissolved in the formalin solution. Potassium channel inhibitors were administered by i.pl. injection in 5 μl of the appropriate vehicle 10 min before formalin. In other experiments, we injected capsaicin, OEA, or other drugs without formalin in a vehicle of 0.9% sterile saline/5% PEG 400/5% Tween 80 (10 μl). After injections, animals were immediately transferred to a transparent observation chamber where pain behavior (time spent licking and biting the injected paw) was continuously monitored for 45 min (phase I: 0–15 min; phase II: 15–45 min) in the formalin experiments and for 15 min in other experiments.

Writhing test. We injected magnesium sulfate (120 mg kg^{-1} in 0.5 ml of saline i.p.) into 12-h food-deprived mice and measured writhing episodes for 30 min. Mechanical hyperalgesia was determined by measuring the latency in seconds to withdraw the paw away from a constant mechanical pressure exerted onto the dorsal surface. A 15-g calibrated glass cylindrical rod (diameter = 10 mm) chambered to a conical point (diameter = 3 mm) was used to exert the mechanical force. The weight was suspended vertically between two rings attached to a stand and was free to move vertically. A cutoff time of 180 s was used. Withdrawal thresholds were measured on both the ipsilateral paw (inflamed or ligated) and contralateral paw (uninflamed or unligated) 30 min after i.p. drug administration for acute experiments or 30 min after s.c. drug administration for chronic experiments. Thermal hyperalgesia was assessed by the method of Hargreaves et al. (1988) by measuring the latency to withdraw the hindpaw from a focused beam of radiant heat (thermal intensity: infrared 3.0) applied to the plantar surface using a plantar test apparatus (Ugo Basile). The cutoff time was set at 30 s. Locomotor performance was assessed using an accelerating rotarod (model 7750; Ugo Basile), which consisted of a base platform and a rotating horizontal rod (7 cm in diameter, 50 cm in length) with a nonskid surface, divided into four sections of equal length to allow for the simultaneous analyses of four mice. A V-shaped counter-trip plate was positioned under each drum section, 26 cm below the rod on the platform. Animals were acclimatized to the revolving drum and habituated to handling to avoid stress during testing. The rod was set to accelerate from 4 to 40 rpm in a 5-min period. The integrity of motor coordination was assessed as the performance time on the rod measured from the start of acceleration until the animal fell from the drum onto the counter-trip plate. Mice were acclimatized to acceleration by three training runs before testing. GW7647 and PEA (each at 30 mg kg^{-1} i.p.) were administrated in a vehicle of 5% PEG, 5% Tween 80, and saline. Rotarod performance was measured at times 0 (basal) and 30 or 60 min after injection of vehicle or GW7647 or PEA. Cutoff was 120 s.

Electrophysiology. Male Sprague-Dawley rats (250–325 g) were anesthetized with urethane (25%, 1.2 g kg^{-1} i.p.), and a laminectomy was performed (Hohmann et al., 1999). Extracellular recordings were made from isolated wide dynamic range (WDR) neurons using tungsten microelectrodes (3 MΩ; FHC Inc., Brunswick, ME). One cell was recorded per animal. WDR neurons were characterized by their responses to mechanical stimulation of the cutaneous receptive field at intensities ranging from non-noxious to noxious levels. An innocuous brush stimulus was applied using an artist brush, and pressure was applied using hemostats. Noxious pinch was applied using an arterial clamp at a fixed intensity deemed noxious by the experimenter. After isolating a single WDR neuron and mapping its receptive field on the plantar surface of the hind paw, each mechanical stimulus was presented for 10 s with a 50-s interstimulus interval.

TABLE 1
Effects of fenofibric acid in the formalin test

Agent	Nocifensive Behavior	
	Phase I	Phase II
	s	
Vehicle	166 ± 19	164 ± 30
Fenofibric acid (100 μg)	121 ± 22	196 ± 27
Fenofibric acid (400 μg)	105 ± 26	144 ± 35
Fenofibric acid (1000 μg)	129 ± 13	153 ± 37

ANOVA, followed by a Dunnett's post hoc test (n = 7–8).

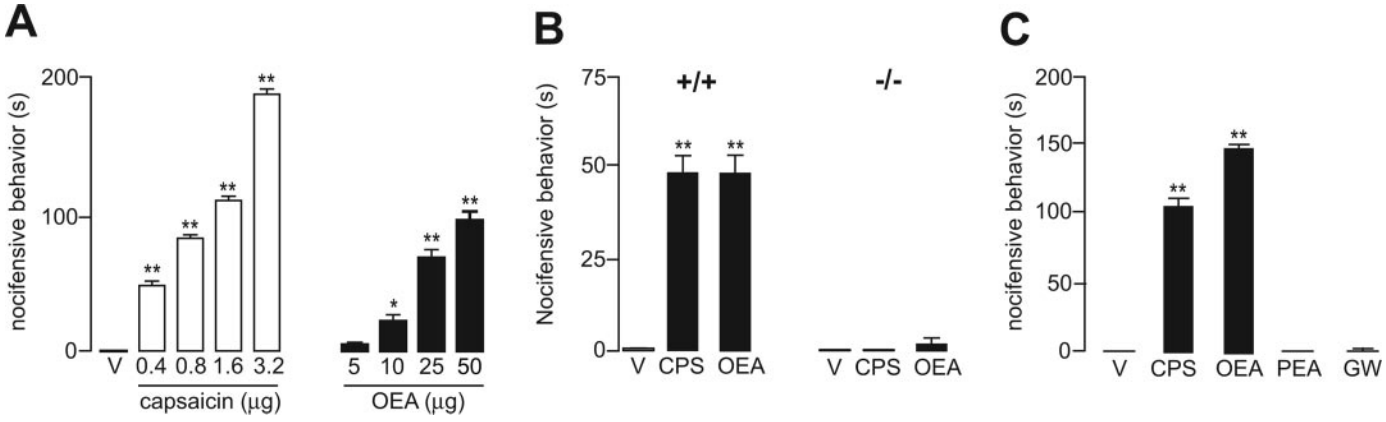

Fig. 2. OEA elicits nocifensive behavior in mice through activation of vanilloid TRPV-1 receptors. A, dose-dependent effects of capsaicin (0.4–3.2 μg i.pl.) or OEA (5–50 μg i.pl.) on nocifensive behaviors in Swiss mice. V, vehicle. B, I.pl. administration of capsaicin (CPS, 1.6 μg) or OEA (50 μg) produces pain behavior in wild-type (+/+), but not TRPV-$1^{-/-}$ (−/−) mice. C, effects of vehicle, capsaicin (CPS, 1.6 μg), OEA (50 μg), PEA (50 μg), and GW7647 (GW, 50 μg) on nocifensive behavior after i.pl injection into the mouse hind paw (n = 4–10). *, $P < 0.05$; **, $P < 0.01$ versus V.

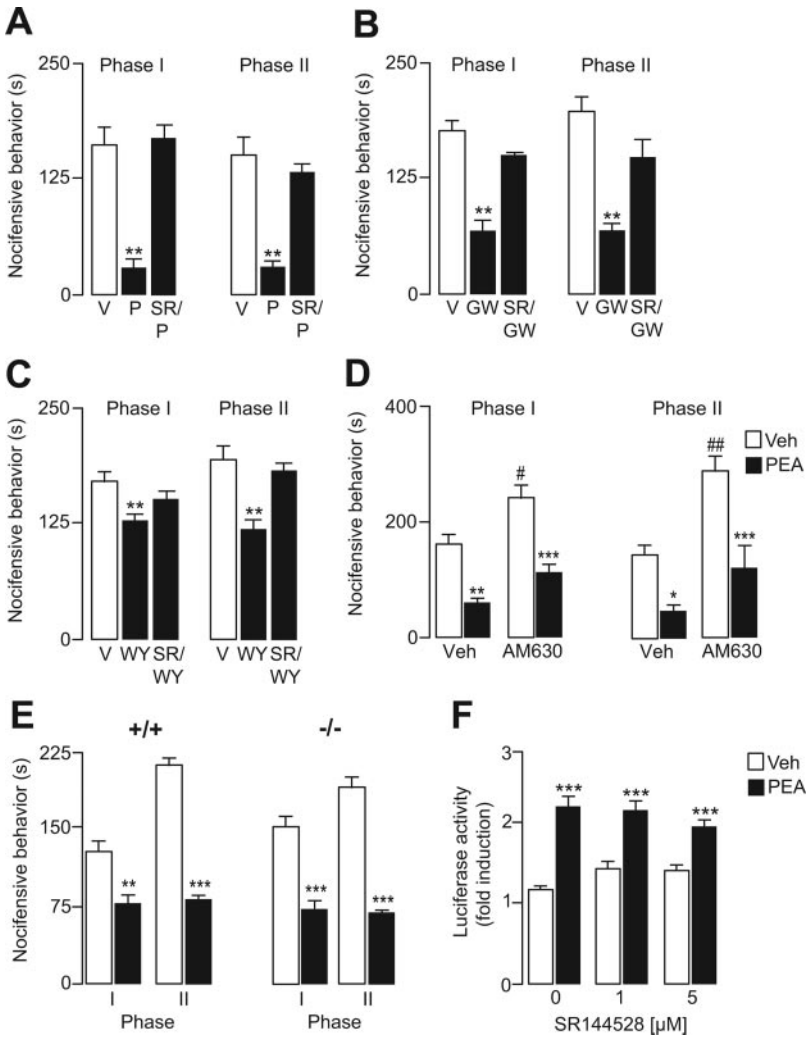

Fig. 3. PPAR-α antinociception does not require CB_2 receptors. A–D, effects of two structurally unrelated CB_2 receptor antagonists, SR144528 and AM630, on PPAR-α-induced antinociception. A–C, effects of vehicle (V), PEA (P, 50 μg i.pl.) (A), GW7647 (GW, 50 μg i.pl.) (B), or Wy-14643 (WY, 100 μg i.pl.) (C), alone or in combination with SR144528 (SR, 1 mg kg^{-1} i.v., 30 min before formalin), on formalin-evoked pain behavior in Swiss mice. SR144528 alone had no effect. D, effects of PEA (50 μg i.pl.), alone or in combination with AM630 (2 mg kg^{-1} i.p., 30 min before formalin), on formalin-evoked pain behavior in Swiss mice. E, effects of vehicle (open bars) or PEA (closed bars, 50 μg i.pl.) on formalin-evoked pain behavior in $CB_2^{-/-}$ (−/−) mice or their wild-type (+/+) littermates (A–E, $n = 6$–10). F, effects of vehicle (open bars) or PEA (closed bars, 10 μM) on PPAR-α activation in the presence or absence of the CB_2 antagonist SR144528 (0–5 μM). Data are expressed as -fold induction of luciferase activity ($n = 4$). ∗, $P < 0.05$; ∗∗, $P < 0.01$; ∗∗∗, $P < 0.001$ versus V.

Spontaneous activity was measured over 1 s immediately before presentation of mechanical stimuli. The oscilloscope and data acquisition system were not in view of the experimenter during application of mechanical stimuli (brush, pressure, and pinch). This procedure served to minimize possible feedback that could otherwise contribute to differences in manual presentation of stimuli and evoked responses. After establishing stable baseline responsiveness to mechanical stimulation, PEA (50 μg; $n = 5$), GW7647 (100 μg; $n = 5$), or vehicle (50 μl; 5% Tween 80:5% PEG 400:90% saline; $n = 9$) was administered into the plantar surface of the hind paw. Responses to mechanical stimulation were reassessed 5 min after injection of drug or vehicle just before i.pl. administration of formalin. In all cases, spontaneous firing returned to preinjection levels before formalin administration or presentation of mechanical stimuli. Responsiveness of WDR neurons to a unilateral i.pl. injection of formalin solution (5% formaldehyde) was subsequently monitored over 60 min. Before termination of recording, responsiveness to cutaneous stimulation was reassessed (~60 min postformalin). Data were collected using a CED 1401 interface and Spike2 software (CED, Cambridge, UK). Action potential waveforms were continuously monitored for size and shape, enabling us to confirm that the same cell was recorded pre- and postformalin. Analyses of electrophysiological data were conducted by repeated measures ANOVA, ANOVA, and Bonferroni's test. The Greenhouse-Geisser correction was applied to all repeated factors to avoid spurious significance due to lack of homogeneity of variance and covariance in repeated factors.

Statistical Analyses

Results are expressed as the mean ± S.E.M. of n experiments. Analyses of data were conducted using Prism software (GraphPad Software, San Diego, CA). The significance of differences between groups was determined by one- or two-way ANOVA followed by a Dunnett's or Bonferroni's test for multiple comparisons, as appropriate. Within-group analysis was conducted with a Student's t test.

Results

PPAR-α Modulates Acute Nociception. We first tested a series of structurally diverse PPAR-α agonists for their ability to reduce the nocifensive behavior caused in mice by i.pl. injection of the chemical irritant formalin. When administered together with formalin, the synthetic PPAR-α agonists GW7647 (reported in vitro human receptor transactivation EC_{50} value: 0.006 μM) (Brown et al., 2001) and Wy-14643 (reported in vitro human receptor transactivation EC_{50} value: 5 μM) (Willson et al., 2000; Brown et al., 2001) reduced both early and late phases of irritant-induced nociception (Fig. 1, A and B). In 10 experiments, the median effective dose (ED_{50}) to prevent early-phase pain behavior was 9.9 μg for GW7647 and 97.0 μg for Wy-14643. As reported previously (Calignano et al., 1998; Jaggar et al., 1998), the natural PPAR-α ligand PEA (reported in vitro human

receptor transactivation EC_{50} value: 3 μM) (LoVerme et al., 2005b) exerted a similar effect (Fig. 1, A and B) (ED_{50} = 7.4 μg), whereas the low-affinity PPAR-α ligand fenofibric acid (reported in vitro human receptor activation EC_{50} value: 30 μM) (Willson et al., 2000; Brown et al., 2001) produced a trend in the reduction of phase I nocifensive behaviors that did not reach statistical significance (Table 1). Notably, GW7647 and PEA did not significantly affect formalin-induced edema formation within the 45-min time frame of the test (Fig. 1C), underscoring the temporal dissociation between the antinociceptive and antiinflammatory effects of these compounds. Marked antinociception was also observed after s.c. administration of GW7647, PEA, or Wy-14643 in a mouse model of acute visceral pain (magnesium sulfate-induced writhing) (Fig. 1I).

The obligatory role of PPAR-α in the antinociceptive effects of PPAR-α agonists was demonstrated by two findings. First, mutant mice lacking the receptor failed to respond to either GW7647 (Fig. 1D) or PEA (Fig. 1, E and J), although they responded normally to the cannabinoid analgesic (*R*)-methanandamide (Fig. 1F). Second, the selective PPAR-δ agonist GW501516 and PPAR-γ agonist ciglitazone did not alter nocifensive behavior in the formalin test (Fig. 1, G and H). The endogenous PPAR-α agonist OEA (Fu et al., 2003) was also inactive (data not shown). However, the lack of PPAR-α-mediated antinociceptive activity of this compound is probably accounted for by its concomitant pronociceptive actions that are mediated by vanilloid TRPV-1 receptors (Ahern, 2003). Indeed, i.pl. administration of OEA, without formalin, elicited marked TRPV-1-dependent nocifensive behavior in mice (Fig. 2, A and B), whereas GW7647 and PEA had no such effect (Fig. 2C).

Even though PEA does not bind to CB_2 cannabinoid receptors, its antinociceptive actions are prevented by the CB_2 antagonist SR144528 (Calignano et al., 1998). We confirmed this finding (Fig. 3A; Table 2) and further noted that SR144528 also reversed the effects of GW7647 and Wy-14643 (Fig. 3, B and C), which like PEA exhibited no significant binding to CB_2 (Table 2). Moreover, we found that (i) a CB_2 antagonist chemically unrelated to SR144528, the compound AM630 (Malan et al., 2001; Ibrahim et al., 2003; Quartilho et al., 2003), did not affect the response to PEA (Fig. 3D) and that (ii) PEA retained its full antinociceptive properties in CB_2-null mice (Fig. 3E). These results demonstrate that SR144528 blocks the antinociceptive effects of PPAR-α agonists by interacting with a site distinct from CB_2. This site remains unidentified but might be located downstream of

TABLE 2
Binding of PPAR-α agonists to human CB_2 receptor

Agent	Concentration	[^{3}H]WIN-55212-2 Binding
	μM	*% of control*
Vehicle		100.0 ± 1.9
GW7647	1	102.1 ± 4.0
	10	91.6 ± 4.1
PEA	1	106.2 ± 2.5
	10	98.5 ± 4.2
Wy-14643	1	104.2 ± 3.6
	10	105.6 ± 1.5
WIN-55212-2	1	4.2 ± 2.2**

** $P < 0.01$, ANOVA, followed by Dunnett's post hoc test (n = 8–9).

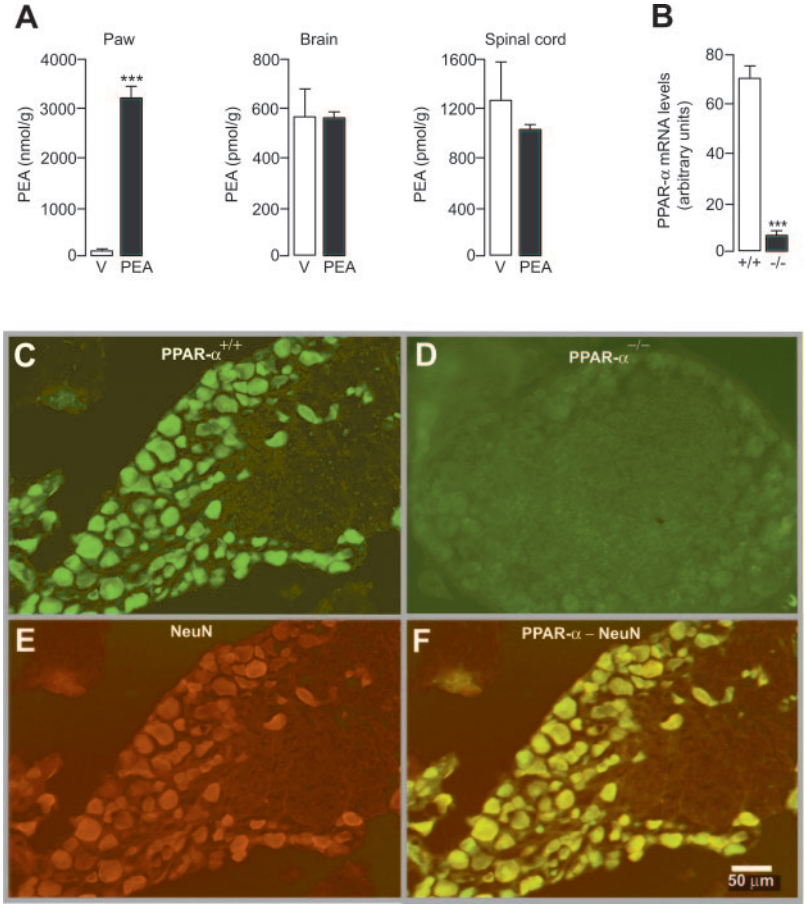

Fig. 4. PPAR-α agonists inhibit nociception through a peripheral mechanism. A, distribution of PEA in paw, brain, and lumbar spinal cord 15 min after a single i.pl. injection of vehicle (V; open bars) or PEA (closed bars; 50 μg) in Swiss mice (n = 5). ***, $P < 0.001$ versus V. B–F, PPAR-α expression in mouse DRG neurons. B, PPAR-α mRNA levels, normalized to GAPDH mRNA levels, in DRG from wild-type (open bars) or PPAR-$\alpha^{-/-}$ mice (closed bars) (n = 5). ***, $P < 0.001$ versus WT. C–F, PPAR-α immunoreactivity (green) in sections of DRG from wild-type C57BL6 mice (C) and PPAR-$\alpha^{-/-}$ mice (D). E, presence of NeuN immunoreactivity (red) in DRG from wild-type C57BL6 mice. F, colocalization of PPAR-α and NeuN immunoreactivity in C57BL6 mice. Scale bars: C–F, 50 μm. The staining shown is representative of multiple sections from five mice.

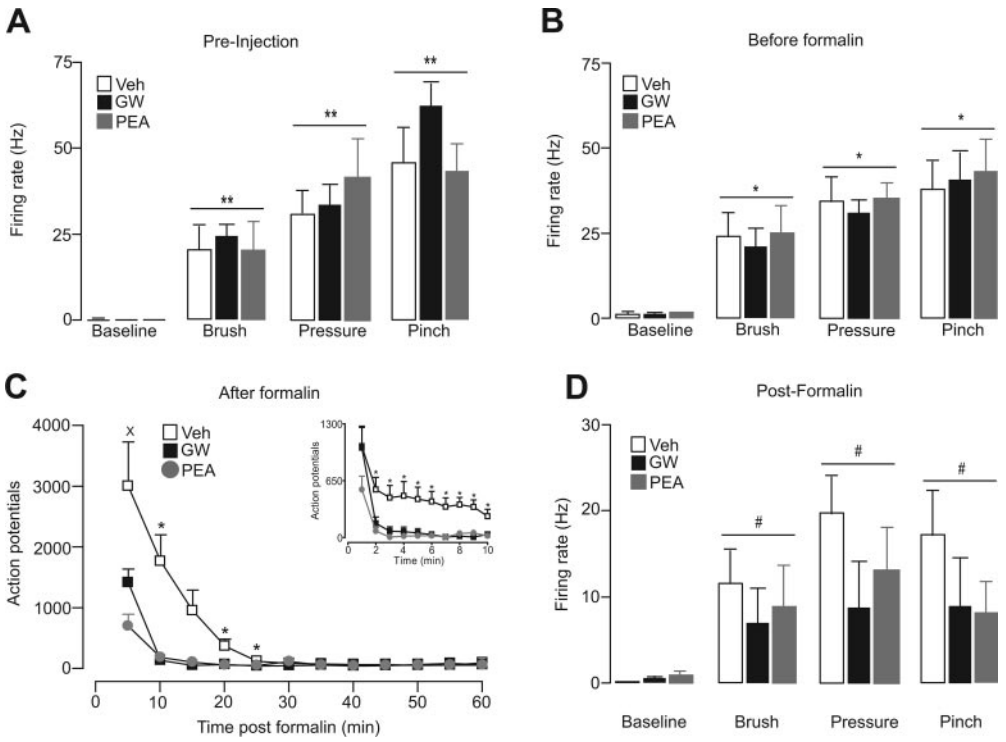

Fig. 5. PPAR-α agonists suppress formalin-induced firing in rat spinal cord nociceptive neurons. A, responses of rat-spinal WDR neurons to cutaneous (brush, pressure, or noxious pinch) stimulation before intraplantar injections for the corresponding treatment groups. B, I.pl. administration of vehicle (open bars, 50 μl), GW7647 (closed bars, 100 μg), or PEA (shaded bars; 50 μg) does not affect neuron firing rate (Hertz) in response to skin stimulation (brush, pressure, and noxious pinch). Baseline levels of spontaneous activity, measured immediately before presentation of mechanical stimuli, are also shown. C, time course of formalin-evoked firing, measured as total number of action potentials per 5-min time bin, in groups of rats after injection of vehicle (open squares), GW7647 (closed squares, 100 μg i.pl.), or PEA (shaded circles, 50 μg i.pl.). Inset, magnification of the first 10 min of the formalin response. D, responses of rat-spinal WDR neurons to cutaneous (brush, pressure, or noxious pinch) stimulation approximately 60 min after formalin injection. For comparison, baseline levels of spontaneous activity before presentation of mechanical stimuli are shown ($n = 5–9$). ∗, $P < 0.05$; ∗∗, $P < 0.01$ versus all other groups; ×, $P < 0.05$ versus PEA; #, $P < 0.05$ versus baseline.

PPAR-α because SR144528 did not significantly antagonize PEA-induced PPAR-α activation in vitro (Fig. 3F).

PPAR-α Agonists Inhibit Nociception through a Peripheral Mechanism. After i.pl. administration of PEA in mice, tissue levels of the drug were markedly elevated in the injected paw but remained unchanged in the brain and lumbar spinal cord (Fig. 4A), indicating that PPAR-α agonists may inhibit pain behavior through a peripheral mechanism. Two observations support this idea. First, mouse DRG (L_4–L_8) were found to contain both PPAR-α mRNA (Fig. 4B) and PPAR-α immunoreactivity (Fig. 4C). The latter was detected in a majority of small and large cells within L_5–L_6 DRG, which were identified as neurons by the presence of the neuronal-specific nuclear protein NeuN (Fig. 4, E and F). As expected, both PPAR-α mRNA and PPAR-α immunoreactivity were detectable in DRG from wild type but not PPAR-α-null mice (Fig. 4, B–D). Second, administration of PPAR-α agonists strongly attenuated the electrophysiological response of spinal nociceptive neurons to peripheral noxious stimuli. We recorded from WDR neurons in the rat spinal cord, whose receptive fields were localized on the plantar surface of the hindpaw ipsilateral to the recording site (Nackley et al., 2004). All recorded neurons were located at similar tissue depths (526.6 ± 81.7, 750.4 ± 40.0, and 543.6 ± 65.33 μm for groups receiving PEA, GW7647 (50 μg), or vehicle, respectively) and exhibited comparable firing rates in response to mechanical stimulation of their cutaneous receptive fields (Fig. 5A). I.pl. administration of PEA or GW7647 did not affect the response to mechanical stimulation before formalin injection (Fig. 5B), indicating a lack of local anesthetic activity, but rapidly suppressed the increase in neuronal firing produced by formalin (Fig. 5C), suggesting that peripheral activation of PPAR-α preferentially suppresses sensitization of spinal WDR neurons. After formalin-induced firing had ceased, all tested cells exhibited similar responses to mechanical stimulation, irrespective of previous treatment (Fig. 5D). These findings indicate that PPAR-α agonists modulate pain through a mechanism that involves peripheral nociceptive neurons.

Calcium-Activated K^+ Channels Mediate PPAR-α Antinociception. The antinociceptive effects of PPAR-α agonists, although dependent on PPAR-α, are too rapid to be mediated by gene expression. Therefore, we considered the alternative possibility that ligand-activated PPAR-α modulates nociception through a nongenomic mechanism. To begin to elucidate this mechanism, we focused first on K^+ channels because of their role in the regulation of sensory neuron excitability and pain sensitivity (Sachs et al., 2004), as well as their involvement in the modulatory effects of PEA in airway hyperreactivity (Yoshihara et al., 2005). Charybdotoxin and clotrimazole, two inhibitors of large-conductance K_{ca} channels (BK_{ca}, $K_{ca}1.1$) and intermediate-conductance K_{ca} channels (IK_{ca}, $K_{ca}3.1$) (Faber and Sah, 2003), prevented the antinociceptive actions of GW7647 and PEA in the formalin test (Fig. 6, A and C) without affecting those of the cannabinoid analgesic (*R*)-methanandamide (Fig. 6, B and

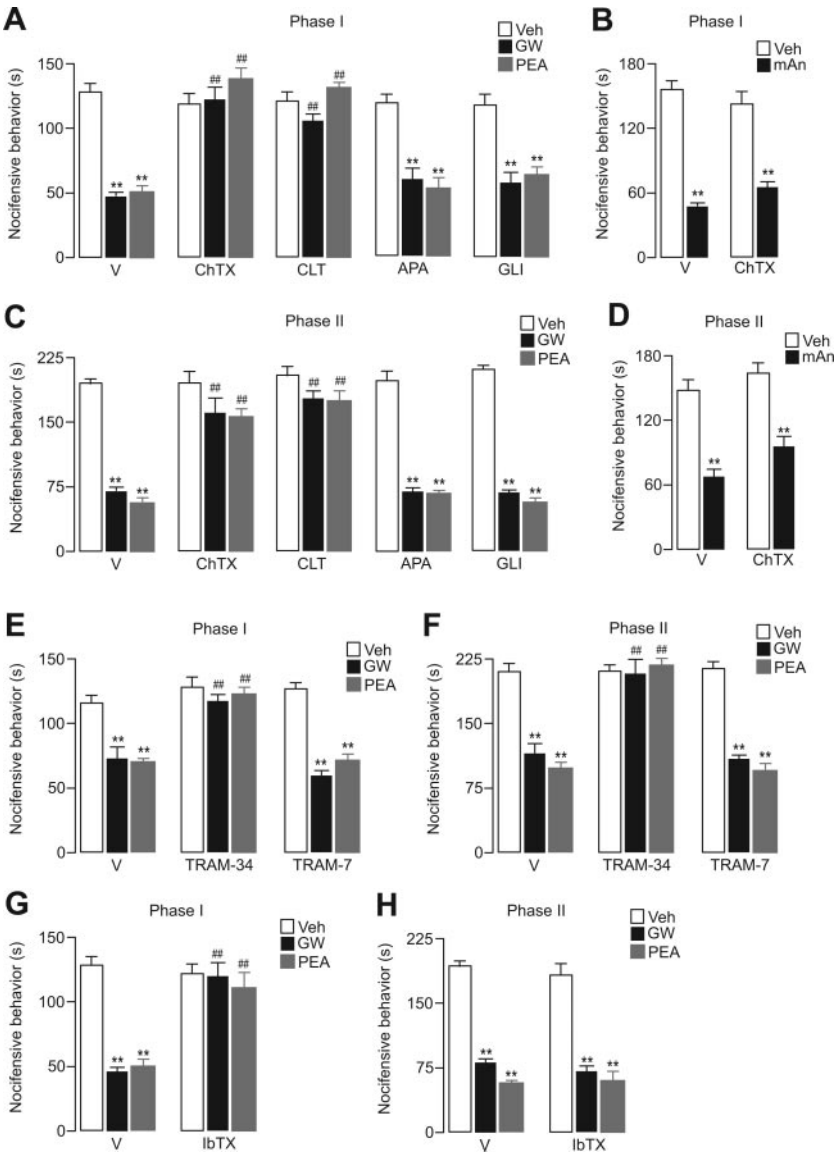

Fig. 6. PPAR-α-induced antinociception requires calcium-activated K^+ channels IK_{ca} and BK_{ca}. A–H, effects of vehicle (V), charybdotoxin (ChTX, 0.5 μg i.pl.) (A–D), clotrimazole (CLT, 5 μg i.pl.), apamin (APA, 1 μg i.pl.), and glibenclamide (GLI, 5 μg i.pl.) (A and C), TRAM-34 (0.5 μg i.pl.) and TRAM-7 (0.5 μg i.pl.) (E and F), or iberiotoxin (IbTX, 0.5 μg i.pl.) (G and H) administered 10 min before vehicle (open bars), GW7647 (closed bars, 50 μg i.pl.), PEA (shaded bars, 50 μg i.pl.) (A, C, E–H), or methanandamide (B and D) on early- (Phase I) (A, B, E, and G) or late-phase (Phase II) (C, D, F, and H) formalin pain in Swiss mice (n = 8–10). **, $P < 0.01$ versus V; ##, $P < 0.01$ versus PEA or GW7647.

D). By contrast, apamin (Faber and Sah, 2003), an inhibitor of small-conductance K_{ca} channels (SK_{ca}, K_{ca}2.1–2.3), and glibenclamide, an inhibitor of ATP-sensitive K^+ channels (K_{ATP}), exerted no such effect (Fig. 6, A and C).

To further delineate the involvement of K_{ca} channels in PPAR-α-mediated antinociception, we used the selective IK_{ca} inhibitor TRAM-34 (Wulff et al., 2000) and the selective BK_{ca} inhibitor iberiotoxin (Faber and Sah, 2003). I.pl. administration of TRAM-34, but not its inactive analog TRAM-7, suppressed the antinociceptive effects of GW7647 and PEA (Fig. 6, E and F). By contrast, iberiotoxin reduced these effects only during the early phase of formalin-induced nociception (Fig. 6, G and H). We interpret the results to indicate that IK_{ca} and BK_{ca} cooperate in mediating different components of the rapid antinociceptive response to PPAR-α agonists.

PPAR-α Agonists Reduce Neuropathic Hyperalgesia. To examine whether PPAR-α agonists attenuate the persistent hyperalgesia associated with nerve injury, we produced peripheral neuropathy in mice by loosely ligating the left sciatic nerve, a surgical procedure that results in the development of mechanical and thermal hyperalgesia in the operated limb (Bennett and Xie, 1988). On days 7 and 14 after surgery, when nocifensive behavior had reached maximal levels, we administered a single i.p. dose of GW7647 or vehicle and, 30 min later, measured their acute effects on pain behavior (Randall and Selitto, 1957; Hargreaves et al., 1988). Administration of GW7647 caused a rapid reversal of both mechanical (Fig. 7A) and thermal (Fig. 7B) hyperalgesia, whereas injections of vehicle were ineffective (Fig. 7, A and B). This antihyperalgesic action was absent in neuropathic PPAR-α-null mice (Fig. 7C). PEA elicited a response similar to that of GW7647 (Fig. 7, D and E), which was also dose-dependent (Fig. 7F) and contingent on PPAR-α expression (Fig. 7G). The antihyperalgesic effects of PPAR-α agonists in this model were comparable to those elicited by gabapentin (Fig. 7, H and I) and were not accompanied by changes in locomotor activity (Table 3) or withdrawal latencies in the noninjected limbs (data not shown).

PPAR-α Agonists Reduce Inflammatory Hyperalgesia. We further explored the ability of PPAR-α agonists to alleviate hyperalgesia in two mouse models of chronic inflammation: (i) experimental arthritis elicited by intradermal in-

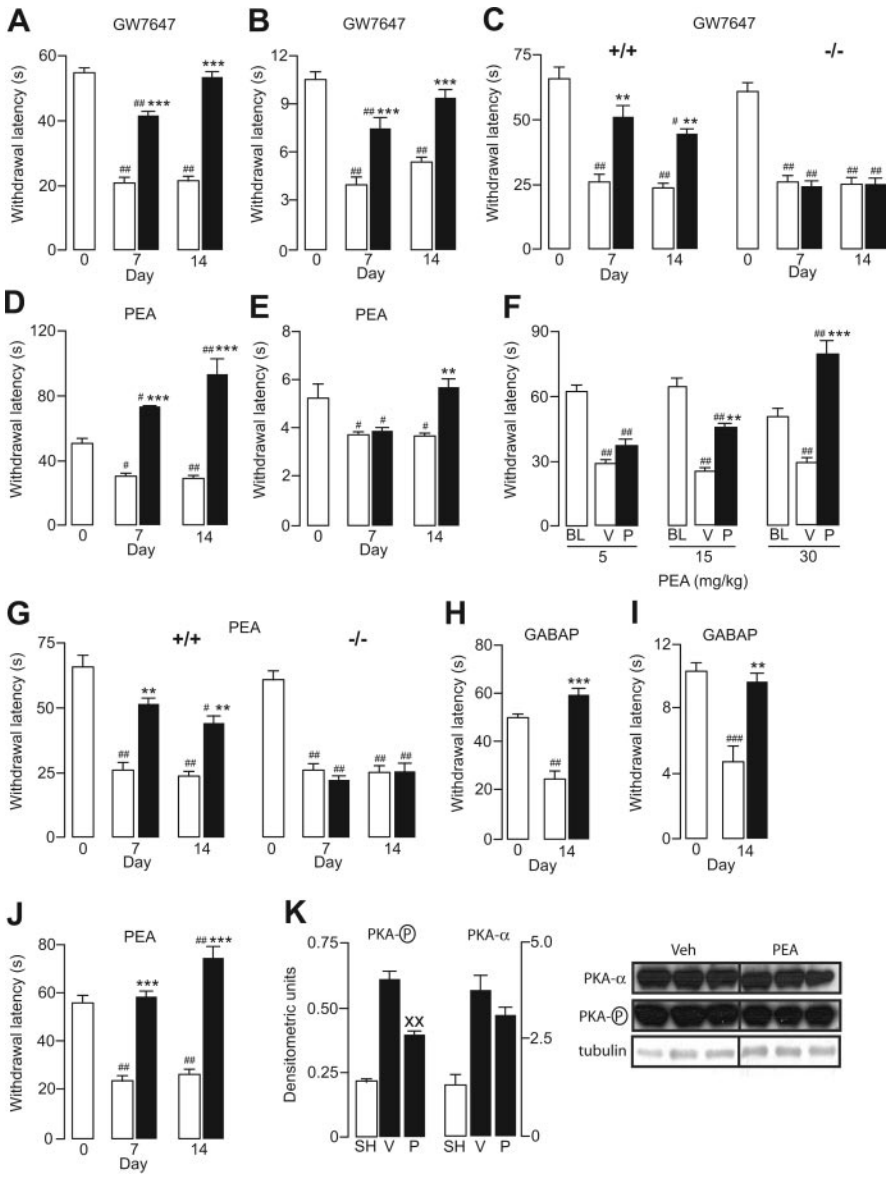

Fig. 7. PPAR-α agonists suppress neuropathic hyperalgesia in mice. A to C, effects of vehicle (open bars) or GW7647 (closed bars) (shaded bars, 30 mg kg^{-1} i.p.) on mechanical (A and C) or thermal withdrawal latencies (B) at days 7 and 14 after sciatic nerve ligation in Swiss mice (A and B) or wild-type C57BL6 (+/+) or PPAR-$\alpha^{-/-}$ (−/−) mice (C). Day 0, baseline responses before surgery (n = 8). D to E, effects of vehicle (open bars) or PEA (closed bars) (shaded bars, 30 mg kg^{-1} i.p.) on mechanical (D) or thermal withdrawal latencies (E) at days 7 and 14 after sciatic nerve ligation in Swiss mice. Day 0, baseline responses before surgery (n = 8). F, dose-dependent effects of PEA administration (5–30 mg kg^{-1} i.p.) on mechanical withdrawal latencies on day 14 after sciatic nerve ligation in Swiss mice. BL, day 0 baseline responses before surgery (n = 6). G, effects of vehicle (open bars) or PEA (closed bars) (shaded bars, 30 mg kg^{-1} i.p.) on mechanical withdrawal latencies at days 7 and 14 after sciatic nerve ligation in wild-type C57BL6 (+/+) or PPAR-$\alpha^{-/-}$ (−/−) mice. Day 0, baseline responses before surgery (n = 8). H and I, effects of vehicle (open bars) or gabapentin (closed bars, 60 mg kg^{-1} i.p.) on mechanical (H) or thermal withdrawal latencies (I) on day 14 after surgery in Swiss mice (n = 6). J, effects of vehicle (open bars) or PEA (closed bars, 30 mg kg^{-1} s.c. once daily for 14 days) on mechanical withdrawal latencies on days 7 and 14 after surgery in Swiss mice (n = 8). K, immunoblot quantification of PKA-IIa regulatory subunit phosphorylation on Ser^{96} and PKA-α catalytic subunit in sham-operated (SH, open bars) or neuropathic (closed bars) Swiss mice treated with vehicle (V) or PEA (P, 30 mg kg^{-1} s.c once daily for 14 days) (n = 3–4). **, $P < 0.01$; ***, $P < 0.001$ versus V; #, $P < 0.05$; ##, $P < 0.01$ versus day 0; ××, $P < 0.01$ versus sham-operated.

TABLE 3
Effects of PPAR-α agonists on rotarod performance 30 or 60 min after vehicle, PEA, or GW7647 (each at 30 mg kg^{-1} i.p.) in Swiss mice (n = 8)

	Latency	
	30 min	60 min
	s	
Veh	109.3 ± 4.6	110.9 ± 4.5
GW7647	109.3 ± 9.9	115.5 ± 3.7
PEA	111.3 ± 5.2	112.5 ± 4.3

jection of CFA into the base of the tail (Whiteley and Dalrymple, 2001) and (ii) paw edema induced by i.pl. injection of carrageenan (Morris, 2003). On days 7 and 14 after CFA injection, when arthritis in both hind limbs was fully developed, we administered a single i.p. dose of GW7647 or PEA and measured pain behavior 30 min later. Either drug, but not their vehicle, suppressed mechanical (Fig. 8, A and C) and thermal (Fig. 8, B and D) hyperalgesia. Likewise, single injections of GW7647 or PEA reduced mechanical and thermal hyperalgesia in the inflamed paws of carrageenan-treated mice (Fig. 8, E–H). Consistent with previous results (Fig. 1C), neither compound affected carrageenan-induced edema within the 30-min test period (Fig. 8I). These results further support the conclusion that ligand-activated PPAR-α suppresses hyperalgesia before alleviating inflammation.

PPAR-α Agonists Do Not Induce Tolerance. The prolonged use of opiate analgesics is often associated with the development of tolerance—the progressive loss of efficacy of a constant dose of drug. To assess whether tolerance develops to the antihyperalgesic effects of PPAR-α agonists, we administered PEA by s.c. injection once a day for 14 consecutive days and measured mechanical and thermal hyperalgesia at days 7 and 14. Neuropathic mice receiving PEA injections exhibited significant mechanical hyperalgesia compared with vehicle-treated mice (Fig. 7J). Paw-withdrawal latency values in the group of mice, subchronically treated with PEA, were similar to those that had received a single PEA injection and remained significantly higher than those of vehicle-treated mice throughout the treatment (Fig. 7J). Immunoblot analyses of lumbar spinal cord extracts revealed that phosphorylation of PKA-IIa regulatory subunit at Ser^{96}, which is

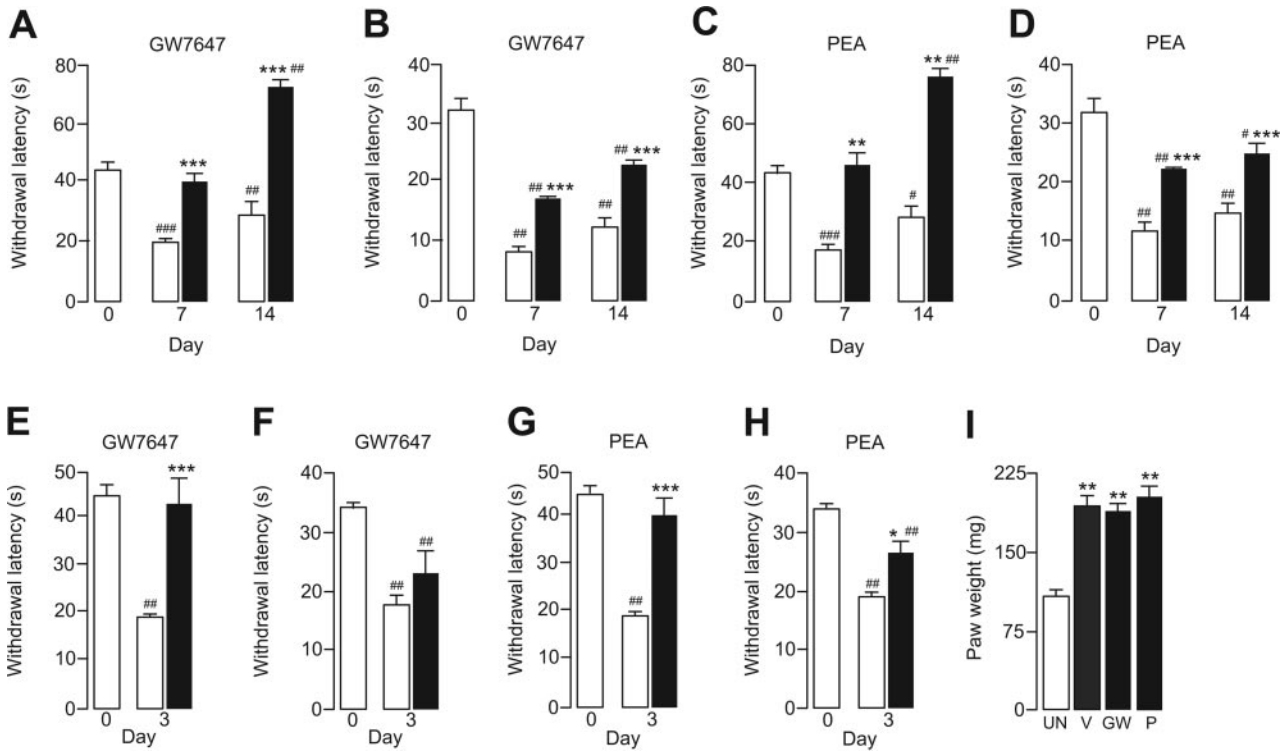

Fig. 8. PPAR-α agonists suppress inflammatory hyperalgesia in mice. A to C, effects of a 30-min pretreatment of vehicle (open bars), GW7647 (closed bars, 30 mg kg^{-1} i.p.) (A and B) or PEA (shaded bars, 30 mg kg^{-1} i.p.) (C and D) on mechanical (A and C) or thermal withdrawal latencies (B and D) on days 7 and 14 after CFA injection in Swiss mice. Day 0, baseline response before CFA injection ($n = 8$). E-I, effects of a 30-min pretreatment of vehicle (open bars), GW7647 (closed bars, 30 mg kg^{-1} i.p.) (E and F), or PEA (shaded bars, 30 mg kg^{-1} i.p.) (G and H) on mechanical (E and G) or thermal withdrawal latencies (F and H) on day 3 after carrageenan injection in Swiss mice. Day 0, baseline response before carrageenan injection ($n = 8$). I, paw edema in carrageenan-treated mice; UN, paw weight in animals not treated with carrageenan ($n = 5$). *, $P < 0.05$; **, $P < 0.01$; ***, $P < 0.001$) versus V; #, $P < 0.05$; ##, $P < 0.01$; ###, $P < 0.001$ versus day 0.

enhanced in neuropathic mice and may contribute to central sensitization (Kawasaki et al., 2004), was reduced in animals treated with PEA compared with vehicle-treated controls (Fig. 7K). Spinal tissue levels of PKA-α catalytic subunit were also slightly decreased by PEA, but this change did not reach statistical significance (Fig. 7K).

Discussion

We have shown that PPAR-α agonists exert rapid and profound antinociceptive effects in animal models of acute, persistent inflammatory, and neuropathic pain, which are contingent on PPAR-α expression. These effects are comparable in time course and magnitude to those elicited by the clinically used analgesic gabapentin and are not associated with the development of tolerance. Thus, our results reveal a previously unsuspected role of PPAR-α in pain modulation and suggest that this nuclear receptor may provide a novel target for broad-spectrum analgesic drugs.

PPAR-α regulates systemic inflammation by inducing the expression of anti-inflammatory proteins, such as IκB-α, repressing the expression of proinflammatory proteins, such as tumor necrosis factor-α, and limiting the recruitment of immune cells to inflammation sites (Kostadinova et al., 2005). This array of effects is mediated through two separate but converging mechanisms—the induction of responsive target genes and the inhibition of transcription factor activities—both of which ultimately involve changes in gene expression. Because these changes unfold over a period of hours or even days, they cannot account for the fast inhibitory actions of PPAR-α agonists on nocifensive behavior and WDR neuron firing, which occur within minutes of drug administration. An alternative possibility, suggested by work with estrogen and vitamin D receptors (Zanello and Norman, 2004; Chambliss et al., 2005), is that ligand-activated PPAR-α modulates nociception by engaging a signal transduction pathway that is independent of transcription. Our pharmacological experiments with K^+ channel inhibitors support this possibility and identify IK_{Ca} and BK_{Ca} as downstream components of the nongenomic PPAR-α signaling pathway implicated in nociceptive regulation. Although the molecular steps that link PPAR-α activation to the gating of IK_{Ca} and BK_{Ca} channels remain undefined, our results raise the possibility that PPAR-α might regulate two complementary aspects of the adaptive response to tissue injury: 1) behavioral avoidance by inhibiting nociception through a fast-onset nongenomic mechanism and 2) tissue repair by dampening inflammation through a slow-onset genomic mechanism.

When they are injected into the paw, PPAR-α agonists do not enter the central nervous system but strongly suppress nocifensive behavior, which suggests that they modulate pain responses by acting at a peripheral site. This conclusion is supported by the presence of PPAR-α in neurons of the DRG, the first relay station for pain signals traveling to the central nervous system, and by the ability of peripherally administered PPAR-α agonists to suppress formalin-evoked sensitization of spinal nociceptive neurons. It is noteworthy, in this regard, that IK_{Ca} and BK_{Ca} channels are also broadly expressed in DRG and other peripheral neurons (Mongan et

al., 2005) where they are thought to control excitability and transmitter release by influencing action potential afterhyperpolarization (Scholz et al., 1998; Zhang et al., 2003; Raffaelli et al., 2004; Davies et al., 2006). Thus, it is tempting to speculate that ligand-activated PPAR-α may suppress pain responses by altering the gating properties of IK_{Ca} and BK_{Ca} channels in DRG neurons. However, the available information does not allow us to exclude additional sites of action of PPAR-α, for example, keratinocytes or other non-neuronal cells involved in pain initiation (Koegel and Alzheimer, 2001; Ibrahim et al., 2003; Marchand et al., 2005).

The broad effectiveness of PPAR-α agonists in animal models of pain suggests a previously unexpected therapeutic action for these drugs. Although fenobric acid (Willson et al., 2000) does not demonstrate analgesic efficacy after acute administration (Table 1), other fibrates as well as new classes of high-affinity PPAR-α ligands have become available (Xu et al., 2003; Singh et al., 2005). These include dual PPAR-α/PPAR-γ modulators (Fagerberg et al., 2005) that, by combining the analgesic and antiinflammatory activity of PPAR-α with the glucose-lowering properties of PPAR-γ, might offer an innovative therapeutic approach to painful diabetic neuropathies, a condition that afflicts more than 30 million people worldwide.

Acknowledgments

We thank Drs. George Chandy and Heike Wulff for kindly supplying TRAM-34 and TRAM-7 and for critically reading the manuscript; Drs. Nancy Buckley and George Kunos for the generous gift of $CB_2^{-/-}$ mice; and Dr. David Luo for help with immunohistochemistry experiments.

References

Ahern GP (2003) Activation of TRPV1 by the satiety factor oleoylethanolamide. *J Biol Chem* **278:**30429–30434.

Astarita G, Rourke BC, Andersen JB, Fu J, Kim JH, Bennett AF, Hicks JW, and Piomelli D (2006) Postprandial increase of oleoylethanolamide mobilization in small intestine of the Burmese python (Python molurus). *Am J Physiol* **290:** R1407–R1412.

Bennett GJ and Xie YK (1988) A peripheral mononeuropathy in rat that produces disorders of pain sensation like those seen in man. *Pain* **33:**87–107.

Brown PJ, Stuart LW, Hurley KP, Lewis MC, Winegar DA, Wilson JG, Wilkison WO, Ittoop OR, and Willson TM (2001) Identification of a subtype selective human PPARα agonist through parallel-array synthesis. *Bioorg Med Chem Lett* **11:**1225–1227.

Calignano A, La Rana G, Giuffrida A, and Piomelli D (1998) Control of pain initiation by endogenous cannabinoids. *Nature (Lond)* **394:**277–281.

Chambliss KL, Simon L, Yuhanna IS, Mineo C, and Shaul PW (2005) Dissecting the basis of nongenomic activation of endothelial nitric oxide synthase by estradiol: role of ERα domains with known nuclear functions. *Mol Endocrinol* **19:**277–289.

Davies PJ, Thomas EA, and Bornstein JC (2006) Different types of potassium channels underlie the long afterhyperpolarization in guinea-pig sympathetic and enteric neurons. *Auton Neurosci* **124:**26–30.

Faber ES and Sah P (2003) Calcium-activated potassium channels: multiple contributions to neuronal function. *Neuroscientist* **9:**181–194.

Fagerberg B, Edwards S, Halmos T, Lopatynski J, Schuster H, Stender S, Stoa-Birketvedt G, Tonstad S, Halldorsdottir S, and Gause-Nilsson I (2005) Tesaglitazar, a novel dual peroxisome proliferator-activated receptor alpha/gamma agonist, dose-dependently improves the metabolic abnormalities associated with insulin resistance in a non-diabetic population. *Diabetologia* **48:**1716–1725.

Fu J, Gaetani S, Oveisi F, LoVerme J, Serrano A, Rodriguez de Fonseca F, Rosengarth A, Luecke H, Di Giacomo B, Tarzia G, et al. (2003) Oleylethanolamide regulates feeding and body weight through activation of the nuclear receptor PPAR-alpha. *Nature (Lond)* **425:**90–93.

Hargreaves K, Dubner R, Brown F, Flores C, and Joris J (1988) A new and sensitive method for measuring thermal nociception in cutaneous hyperalgesia. *Pain* **32:** 77–88.

Hohmann AG, Tsou K, and Walker JM (1999) Cannabinoid suppression of noxious heat-evoked activity in wide dynamic range neurons in the lumbar dorsal horn of the rat. *J Neurophysiol* **81:**575–583.

Ibrahim MM, Deng H, Zvonok A, Cockayne DA, Kwan J, Mata HP, Vanderah TW, Lai J, Porreca F, Makriyannis A, et al. (2003) Activation of CB_2 cannabinoid receptors by AM1241 inhibits experimental neuropathic pain: pain inhibition by receptors not present in the CNS. *Proc Natl Acad Sci USA* **100**:10529–10533.

Jaggar SI, Hasnie FS, Sellaturay S, and Rice AS (1998) The anti-hyperalgesic actions of the cannabinoid anandamide and the putative CB_2 receptor agonist palmitoylethanolamide in visceral and somatic inflammatory pain. *Pain* **76:**189–199.

Kawasaki Y, Kohno T, Zhuang ZY, Brenner GJ, Wang H, Van Der Meer C, Befort K, Woolf CJ, and Ji RR (2004) Ionotropic and metabotropic receptors, protein kinase A, protein kinase C, and Src contribute to C-fiber-induced ERK activation and cAMP response element-binding protein phosphorylation in dorsal horn neurons, leading to central sensitization. *J Neurosci* **24:**8310–8321.

Koegel H and Alzheimer C (2001) Expression and biological significance of Ca^{2+}-activated ion channels in human keratinocytes. *FASEB J* **15:**145–154.

Kostadinova R, Wahli W, and Michalik L (2005) PPARs in diseases: control mechanisms of inflammation. *Curr Med Chem* **12:**2995–3009.

LoVerme J, Fu J, Astarita G, La Rana G, Russo R, Calignano A, and Piomelli D (2005a) The nuclear receptor peroxisome proliferator-activated receptor-alpha mediates the anti-inflammatory actions of palmitoylethanolamide. *Mol Pharmacol* **67:**15–19.

LoVerme J, La Rana G, Russo R, Calignano A, and Piomelli D (2005b) The search for the palmitoylethanolamide receptor. *Life Sci* **77:**1685–1698.

Malan TP Jr, Ibrahim MM, Deng H, Liu Q, Mata HP, Vanderah T, Porreca F, and Makriyannis A (2001) CB_2 cannabinoid receptor-mediated peripheral antinociception. *Pain* **93:**239–245.

Marchand F, Perretti M, and McMahon SB (2005) Role of the immune system in chronic pain. *Nat Rev Neurosci* **6:**521–532.

Mazzari S, Canella R, Petrelli L, Marcolongo G, and Leon A (1996) *N*-(2-Hydroxyethyl)hexadecanamide is orally active in reducing edema formation and inflammatory hyperalgesia by down-modulating mast cell activation. *Eur J Pharmacol* **300:**227–236.

Mongan LC, Hill MJ, Chen MX, Tate SN, Collins SD, Buckby L, and Grubb BD (2005) The distribution of small and intermediate conductance calcium-activated potassium channels in the rat sensory nervous system. *Neuroscience* **131:**161–175.

Morris CJ (2003) Carrageenan-induced paw edema in the rat and mouse. *Methods Mol Biol* **225:**115–121.

Nackley AG, Zvonok AM, Makriyannis A, and Hohmann AG (2004) Activation of cannabinoid CB_2 receptors suppresses C-fiber responses and windup in spinal wide dynamic range neurons in the absence and presence of inflammation. *J Neurophysiol* **92:**3562–3574.

Quartilho A, Mata HP, Ibrahim MM, Vanderah TW, Porreca F, Makriyannis A, and Malan TP Jr (2003) Inhibition of inflammatory hyperalgesia by activation of peripheral CB2 cannabinoid receptors. *Anesthesiology* **99**:955–960.

Raffaelli G, Saviane C, Mohajerani MH, Pedarzani P, and Cherubini E (2004) BK potassium channels control transmitter release at CA3-CA3 synapses in the rat hippocampus. *J Physiol (Lond)* **557:**147–157.

Randall LO and Selitto JJ (1957) A method for measurement of analgesic activity on inflamed tissue. *Arch Int Pharmacodyn Ther* **111:**409–419.

Sachs D, Cunha FQ, and Ferreira SH (2004) Peripheral analgesic blockade of hypernociception: activation of arginine/NO/cGMP/protein kinase G/ATP-sensitive K^+ channel pathway. *Proc Natl Acad Sci USA* **101:**3680–3685.

Scholz A, Gruss M, and Vogel W (1998) Properties and functions of calcium-activated K^+ channels in small neurones of rat dorsal root ganglion studied in a thin slice preparation. *J Physiol (Lond)* **513:**55–69.

Singh JP, Kauffman R, Bensch W, Wang G, McClelland P, Bean J, Montrose C, Mantlo N, and Wagle A (2005) Identification of a novel selective peroxisome proliferator-activated receptor alpha agonist, 2-methyl-2-(4-{3-[1-(4-methylbenzyl)-5-oxo-4,5-dihydro-1*H*-1,2,4-triazol-3- yl]propyl}phenoxy)propanoic acid (LY518674), that produces marked changes in serum lipids and apolipoprotein A-1 expression. *Mol Pharmacol* **68:**763–768.

Taylor BK, Dadia N, Yang CB, Krishnan S, and Badr M (2002) Peroxisome proliferator-activated receptor agonists inhibit inflammatory edema and hyperalgesia. *Inflammation* **26:**121–127.

Whiteley PE and Dalrymple SA (2001) Models of inflammation: adjuvant-induced arthritis in the rat, in *Current Protocols in Pharmacology* (Enna SJ ed) pp 5.5.1–5.5.5, John Wiley & Sons, Inc., New York.

Willson TM, Brown PJ, Sternbach DD, and Henke BR (2000) The PPARs: from orphan receptors to drug discovery. *J Med Chem* **43:**527–550.

Wulff H, Miller MJ, Hansel W, Grissmer S, Cahalan MD, and Chandy KG (2000) Design of a potent and selective inhibitor of the intermediate-conductance Ca^{2+}-activated K^+ channel, $IK_{Ca}1$: a potential immunosuppressant. *Proc Natl Acad Sci USA* **97:**8151–8156.

Xu Y, Mayhugh D, Saeed A, Wang X, Thompson RC, Dominianni SJ, Kauffman RF, Singh J, Bean JS, Bensch WR, et al. (2003) Design and synthesis of a potent and selective triazolone-based peroxisome proliferator-activated receptor alpha agonist. *J Med Chem* **46:**5121–5124.

Yoshihara S, Morimoto H, Ohori M, Yamada Y, Abe T, and Arisaka O (2005) Endogenous cannabinoid receptor agonists inhibit neurogenic inflammations in guinea pig airways. *Int Arch Allergy Immunol* **138:**80–87.

Zanello LP and Norman AW (2004) Rapid modulation of osteoblast ion channel responses by $1\alpha,25(OH)_2$-vitamin D_3 requires the presence of a functional vitamin D nuclear receptor. *Proc Natl Acad Sci USA* **101:**1589–1594.

Zhang XF, Gopalakrishnan M, and Shieh CC (2003) Modulation of action potential firing by iberiotoxin and NS1619 in rat dorsal root ganglion neurons. *Neuroscience* **122:**1003–1011.

Address correspondence to: Dr. Daniele Piomelli, Department of Pharmacology, University of California, Irvine, 360 MSRII, Irvine, CA 92697-4625. E-mail: piomelli@uci.edu